About Some Computational Algorithms for Locally Approximation Splines, Based on the Wavelet Transformation and Convolution

G. Y. Deniskina(✉), Y. I. Deniskin, and Y. I. Bityukov

Moscow Aviation Institute, 4 Volokolamskoye Highway, Moscow 125993, Russian Federation
deniskinagy@gmail.com

Abstract. Currently, the problems of improving the methods of geometric modeling of three-dimensional objects using the standard mathematical apparatus for CAD/CAE/CAM systems, as well as adapting these methods for specific industrial applications, are urgent. In this paper, we consider issues related to obtaining algorithms for finding the values of a locally approximating spline of two variables and its partial derivatives using a discrete wavelet transform and a convolution operation. The considered inverse discrete wavelet transform and convolution transform are applied to finding computational algorithms for local approximation splines, and then applying them to the development of a CAD system for manufacturing structures from composite materials by the method of automated calculation. Also, the results obtained can be used to solve problems associated with local modification of the surface of a fan blade made of composite materials by the method of automated calculation. In this case, the surface of the fan blade is defined by some sets of points in several sections. First, we model this surface using a local approximation spline of two variables. Then we find the values of this spline at the nodes of the finer mesh and shift the surface points corresponding to these nodes along the normal to the surface by a height equal to the thickness of the tape. Next, we carry out the wavelet decomposition with zeroing the wavelet coefficients. As a result, the surface is smoothed.

Keywords: Local approximation spline · Surface modification · Automated layout · CAD/CAM/CAE/PDM systems · Pinch rollers

1 Introduction

Currently, enterprises engaged in the design and manufacture of complex equipment are actively using CAD/CAM/CAE/PDM systems to control the quality of products. In these systems, increased attention is paid to improving the technology of geometric three-dimensional modeling. The main problem is not the modeling process itself, but the methods of modifying and optimizing the created geometric models, which is very critical during the iterative mode of the designer. Therefore, today, the problems of improving the methods of geometric modeling of three-dimensional objects using the mathematical apparatus standard for CAD/CAE/CAM systems, as well as the adaptation of these methods for specific industrial applications, are relevant. Recently, wavelets have been used in

A. A. Radionov and V. R. Gasiyarov (Eds.): RusAutoConf 2020, LNEE 729, pp. 182–191, 2021.
https://doi.org/10.1007/978-3-030-71119-1_19

many problems of geometric modeling, mainly in computer graphics [1, 2]. In this article, the inverse discrete wavelet transform and convolution transform are applied to finding computational algorithms for locally approximating splines [3], and then applying them to the development of a CAD system for manufacturing structures from composite materials by automated calculation.

2 Veivlets on the Segment and Rectangle

For geometric applications we will consider actual spaces $L_2(R)$ and $L_2[a; b]$. Let's take a look at the actual features defined on the segment $[a; b]$. Let the function $\varphi \in L_2(R)$ satisfy the large-scale ratio [4].

$$\varphi(x) = \sqrt{2}\sum_{k\in Z} u_k \varphi(2x-k),\ u_k \in R$$

and has a compact medium. Let's denote $\varphi_{jk}(x) = \varphi(2^j x - k), x \in [a; b], j, k \in Z$. It is clear that for everyone j different from zero on the segment $[a; b]$ will be only the final number of such functions. Let these be functions for certainty $\varphi_{j,0}, \varphi_{j,1}, \ldots, \varphi_{j,n_j-1}$.

Let's take a look [4] at the sequence $V_0 \subset V_1 \subset \ldots$ of space subspaces $L_2[a; b]$.

$$V_j = lin\left\{\varphi_{j,0}, \varphi_{j,1}, \ldots, \varphi_{j,n_j-1}\right\} = \left\{\sum_{s=0}^{n_j-1} a_s\varphi_{j,s}: \quad a_s \in R, s = 0, 1, \ldots, n_j - 1\right\}, \dim V_j = n_j$$

Because $V_{j-1} \subset V_j$, then $\varphi_{j-1,k} = \sum\limits_{s=0}^{n_j-1} p_{s,k}^j \varphi_{j,s}$. Let's introduce the designations [4].

$$\Phi_j(x) = \left(\varphi_{j,0}(x)\ \varphi_{j,1}(x)\ \ldots\ \varphi_{j,n_j-1}(x)\right), P_j = (p_{s,k}^j)_{s=0,k=0}^{n_j-1,\ n_{j-1}-1}$$

Then $\Phi_{j-1} = \Phi_j P_j$. Let's designate the symbol W_{j-1} as an orthogonal addition to space V_{j-1} in space V_j because $V_j = V_{j-1} \oplus W_{j-1}$ and $W_{j-1} \subset V_j$, then W_{j-1} the ultimate space. If $W_j = lin\left\{\psi_{j,0}, \psi_{j,1}, \ldots, \psi_{j,m_j-1}\right\}$, $\dim W_j = m_j$, then $\psi_{j-1,k} = \sum\limits_{s=0}^{n_j-1} q_{s,k}^j \varphi_{j,s}$. Functions $\psi_{j,k}$ are called veilets, and spaces W_j are called veilet spaces [4].

$$\Psi_j(x) = \left(\psi_{j,0}(x)\ \psi_{j,1}(x)\ \ldots\ \psi_{j,m_j-1}(x)\right),$$
$$Q_j = (q_{s,k}^j)_{s=0,k=0}^{n_j-1,m_{j-1}-1}.$$

Then $\Psi_{j-1} = \Phi_j Q_j$. It should be noted that. $n_j + m_j = n_{j+1}$.

Let it be $f \in L_2[a; b]$ and $\Pi_j : L_2[a; b] \to V_j$ projector. Then the approximation $\Pi_j f$ can be decomposed into a rougher approximation $\Pi_{j-1} f$ and clarifying the stoic $\Pi_{j-1}^W f$.

$$\Pi_j f = \sum_{k=0}^{n_j-1} c_{j,k}\varphi_{j,k} = \Pi_{j-1} f + \Pi_{j-1}^W f = \sum_{k=0}^{n_{j-1}-1} c_{j-1,k}\varphi_{j-1,k} + \sum_{k=0}^{m_{j-1}-1} d_{j-1,k}\psi_{j-1,k}.$$

Let's introduce two vectors of coefficients into the review.

$$C_j = \left(c_{j,0} \ldots c_{j,n_j-1} \right)^T, D_j = \left(d_{j,0} \ldots d_{j,n_j-1} \right)^T.$$

The first vector describes the approximation of a function f, and the second vector is a veilet-coefficient that characterizes deviation $\Pi_{j-1}f$ from $\Pi_j f$ [4].

$$C_j = P_j C_{j-1} + Q_j D_{j-1}.$$

On this equality it is possible to restore $\Pi_j f$ the approach on a rougher approach $\Pi_{j-1}f$ and veilet-coefficents. Because line operators (projectors) $V_j \to V_{j-1}$ are $V_j \to W_{j-1}$ defined by some matrix A_j, B_j, then $C_{j-1} = A_j C_j, D_{j-1} = B_j C_j$. By the function's f vevlet transformation, we will understand the location of vectors $C_0, D_0, D_1, \ldots, D_{j-1}$. The relationship [4] between the matrix A_j, B_j and the P_j, Q_j.

$$\begin{pmatrix} A_j \\ B_j \end{pmatrix} = \left(P_j \; Q_j \right)^{-1}.$$

The matrix in Q_j the article [4] is defined from a homogeneous system of linear equations $\mathrm{T}_j\mathrm{Q}_j = 0$, where $\mathrm{T}_j = \mathrm{P}_j^T[(\Phi_j, \Phi_j)]$, as well $[(\Phi_j, \Phi_j)] = ((\varphi_{j,i}, \varphi_{j,s}))_{i,s=0}^{n_j-1}$ - the matrix of scalar works. Matrices Q_j and P_j are known as synthesis filters. Matrices A_j and B_j are known as analysis filters. The set $\{\mathrm{P}_j, \mathrm{Q}_j, \mathrm{A}_j, \mathrm{B}_j\}$ is called a filter bank.

About the above-written approach to building a veilet system on a segment in the article [5] is applied to the case when the function $\varphi(x)$ is chosen B-spline of arbitrary order n. Define the B-splines of the order as n a convolution [6]

$$N_n = N_{n-1} * N_0, N_0(x) = \begin{cases} 1, & x \in [0; 1), \\ 0, & x \notin [0; 1). \end{cases}$$

Note some of the well-known properties of B-splines [6]. Second, $N_n(x) \geq 0$ as shown x in the feature supp $N_n(x) = [0; n+1]$, As shown in [6], the function $N_n(x)$, satisfies the scale ratio

$$N_n(x) = \sum_{k=0}^{n+1} \frac{p_k}{2^n} N_n(2x-k), p_k = C_{n+1}^k = \frac{(n+1)!}{k!(n+1-k)!}. \quad (1)$$

In addition, the function $N_n(x)$ satisfies the ratio of [6]

$$N_n(x) = \frac{x}{n} N_{n-1}(x) + \frac{n+1-x}{n} N_{n-1}(x-1) \quad (2)$$

and justly equality [6].

$$N'_{n+1}(x) = N_n(x) - N_n(x-1). \quad (3)$$

In article [5], the filter bank is built for the case $\varphi(x) = N_n(x)$.

Consider now the use of veilet systems on the segment to build two-dimensional veiwelets on a rectangular area. Let the sequences $V_{0,i} \subset V_{1,i} \subset \ldots V_{j,i} \subset$ of the

final subspaces of space $L_2[a_i; b_i]$ scale functions φ^i and banks of filters $P_{j,i}$, $Q_{j,i}$, $A_{j,i}$, $B_{j,i}$, $i = 1, 2$. The standard approach [7] to the construction of multidimensional wavelet systems is to take tensor products of basis functions from $V_{j,i}$. Define subspaces $V_j^2 = V_{j,1} \otimes V_{j,2} = lin\{f_1 \otimes f_2 : f_1 \in V_{j,1}, f_2 \in V_{j,2}\}$, where the function $f_1 \otimes f_2$ is defined by the rule $f_1 \otimes f_2(x, y) = f_1(x) f_2(y)$. In addition, we define spaces W_j^2 as follows $V_j^2 = V_{j-1}^2 \oplus W_{j-1}^2$. Then, if $f \in L_2([a_1; b_1] \times [a_2; b_2])$ and $\Pi_j : L_2([a_1; b_1] \times [a_2; b_2]) \to V_j^2$ is a projector, then

$$\Pi_j f = \sum_{m=0}^{n_{j,1}-1} \sum_{l=0}^{n_{j,2}-1} c_{m,l}^j \varphi_{j,m}^{(1)} \otimes \varphi_{j,l}^{(2)} = \sum_{m=0}^{n_{j,1}-1} \sum_{l=0}^{n_{j,2}-1} \left(\sum_{k=0}^{n_{j-1,1}-1} \sum_{s=0}^{n_{j-1,2}-1} c_{k,s}^{j-1} p_{m,k}^{j,1} p_{l,s}^{j,2} \right.$$

$$\left. + \sum_{k=0}^{m_{j-1,1}-1} \sum_{s=0}^{n_{j-1,2}-1} r_{k,s}^{j-1} q_{m,k}^{j,1} p_{l,s}^{j,2} + \sum_{k=0}^{n_{j-1,1}-1} \sum_{s=0}^{m_{j-1,2}-1} h_{k,s}^{j-1} p_{m,k}^{j,1} q_{l,s}^{j,2} + \sum_{k=0}^{m_{j-1,1}-1} \sum_{s=0}^{m_{j-1,2}-1} d_{k,s}^{j-1} q_{m,k}^{j,1} q_{l,s}^{j,2} \right) \varphi_{j,m}^{(1)} \otimes \varphi_{j,l}^{(2)}. \tag{4}$$

If you introduce the matrix $C_j = (c_{m,l}^j)_{m,l=0}^{n_{j,1}-1, n_{j,2}-1}$, $R_j = (r_{k,s}^j)_{k,s=0}^{m_{j,1}-1,\ n_{j,2}-1}$, $H_j = (h_{k,s}^j)_{k,s=0}^{n_{j,1}-1,\ m_{j,2}-1}$, $D_j = (d_{k,s}^j)_{k,s=0}^{m_{j,1}-1,\ m_{j,2}-1}$, into consideration (1), we get it from equality [5]

$$C_j = P_{j,1} C_{j-1} P_{j,2}^T + Q_{j,1} R_{j-1} P_{j,2}^T + P_{j,1} H_{j-1} Q_{j,2}^T + Q_{j,1} D_{j-1} Q_{j,2}^T \tag{5}$$

It is also obvious [5] that

$$C_{j-1} = A_{j,1} C_j A_{j,2}^T; R_{j-1} = B_{j,1} C_j A_{j,2}^T; H_{j-1} = A_{j,1} C_j B_{j,2}^T; D_{j-1} = B_{j,1} C_j B_{j,2}^T \tag{6}$$

Formulas (6) give the veilet decomposition of the approximate $\Pi_j f$ function of two arguments, and formula (5) gives a veilet-resolution.

3 Computational Algorithms for Locally Approximates

In this section, we obtained some computational formulas for local approximation spline in narrow grids based on wavelet recovery. The obtained formulas will be used in the approximate calculation of integral data obtained in various grids [8].

Consider the following B-splines

$$N_{l,m,i}(x) = N_{m-1}(2^l x + m - i),\ l, i \in Z,\ m = 1, 2, \ldots$$

Note some of the obvious properties of these features.

Lemma 1. There is equality

$$N_{l,m,i}(x) = N_{l,m,m}(x + 2^{-l}(m - i)) \tag{7}$$

Proof. We have

$$N_{l,m,m}(x + 2^{-l}(m - i)) = N_{m-1}(2^l(x + 2^{-l}(m - i))) = N_{m-1}(2^l x + m - i) = N_{l,m,i}(x).$$

Lemma 2. There is equality

$$N_{0,m,m}(2^l x + k) = N_{l,m,m-k}(x) \tag{8}$$

Proof. We have

$$N_{l,m,m-k}(x) = N_{m-1}(2^l x + k) = N_{0,m,m}(2^l x + k).$$

Lemma 3. Functions $N_{l,m,i}(x)$ satisfy the following Cox – de Boer relation [8].

$$N_{l,m,i}(x) = \frac{i - 2^l x}{m-1} N_{l,m-1,i}(x) + \frac{2^l x - i + m}{m-1} N_{l,m-1,i-1}(x); \tag{9}$$

$$N_{l,1,i}(x) = \begin{cases} 1, x \in \left[\frac{i-1}{2^l}, \frac{i}{2^l}\right); \\ 0, x \notin \left[\frac{i-1}{2^l}, \frac{i}{2^l}\right). \end{cases}$$

Fair equality

$$N'_{l,m,i}(x) = 2^l \cdot N_{l,m-1,i-1}(x) - 2^l \cdot N_{l,m-1,i}(x). \tag{10}$$

Proof. From equality (2) we get

$$N_{l,m,i}(x) = N_{m-1}(2^l x + m - i) = \frac{2^l x + m - i}{m-1} N_{m-2}(2^l x + m - i)$$
$$+ \frac{m - (2^l x + m - i)}{m-1} N_{m-2}(2^l x + m - i - 1).$$

Given that $N_{m-2}(2^l x + m - i) = N_{l,m-1,i-1}(x), N_{m-2}(2^l x + m - i - 1) = N_{l,m-1,i}(x)$ we get the approval of the lemma. Equality (10) follows from equality (3).

Lemma 4. The function $N_{0,m,m}$ satisfies a large-scale ratio.

$$N_{0,m,m}(x) = \sum_{k=0}^{m} \frac{p_k}{2^{m-1}} N_{0,m,m}(2x - k), \; p_k = \frac{m!}{k!(m-k)!} \tag{11}$$

Proof. From (1) follows

$$N_{0,m,m}(x) = N_{m-1}(x) = \sum_{k=0}^{m} \frac{p_k}{2^{m-1}} N_{m-1}(2x - k) = \sum_{k=0}^{m} \frac{p_k}{2^{m-1}} N_{1,m,m+k}(x)$$

From equality (8) we get $N_{1,m,m+k}(x) = N_{0,m,m}(2^l x - k)$.

Lemma 5. The function $N_{l,m,i}(x)$ satisfies the ratio

$$N_{l,m,i}(x) = \sum_{k=0}^{m} \frac{p_k}{2^{m-1}} N_{l+1,m,2i+k-m}(x). \tag{12}$$

Proof. From (8) follows. $N_{l,m,i}(x) = N_{0,m,m}(2^l x + m - i)$ from here, on the basis (11), conclude

$$N_{l,m,i}(x) = \sum_{k=0}^{m} \frac{p_k}{2^{m-1}} N_{0,m,m}(2(2^l x + m - i) - k) = \sum_{k=0}^{m} \frac{p_k}{2^{m-1}} N_{0,m,m}(2^{l+1} x + (2m - 2i - k))$$
$$= \sum_{k=0}^{m} \frac{p_k}{2^{m-1}} N_{l+1,m,2i+k-m}(x).$$

Let $M : Z^2 \to R$. We will also $M(k_1, k_2)$ use the designation for values M_{k_1,k_2}. Let's define the function with $M^- : Z^2 \to R$ equality $M^-_{k_1,k_2} = M_{-k_1,-k_2}$.

Definition 1. Let and $M : Z^2 \to R, F : Z^2 \to R$ – two functions with compact carriers. The convolution $M * F$ of these functions is defined by the equality.

$$(M * F)_{\lambda,\rho} = \sum_{k_1,k_2=-\infty}^{+\infty} M_{k_1,k_2} F_{\lambda-k_1,\ \rho-k_2}$$

We will call M the function the core of the bundle.

Consider the case $m = 4$. Then the ratio (12) will take the form

$$N_{l,4,i}(x) = \frac{1}{8} N_{l+1,4,2i-4}(x) + \frac{1}{2} N_{l+1,4,2i-3}(x) + \frac{3}{4} N_{l+1,4,2i-2}(x) + \frac{1}{2} N_{l+1,4,2i-1}(x) + \frac{1}{8} N_{l+1,4,2i}(x)$$

Suppose the values $f_{k_1,k_2} = f\left(u_{j,k_1,k_2}\right)$, $k_1, k_2 \in Z$ functions $f(u_1, u_2)$ are known in nodes from the site.

$$u_{j,k_1,k_2} = \left(2^{-j} k_1, 2^{-j} k_2\right),$$

$$k_1 = k_{j,1,0} - 2, k_{j,1,0} - 1, \ldots, k_{j,1,1} + 2;$$
$$k_2 = k_{j,2,0} - 2, k_{j,2,0} - 1, \ldots, k_{j,2,1} + 2.$$

The local approximation spline $\tilde{f}$ is determined by the equality [9].

$$\tilde{f}(u_1, u_2) = \sum_{\lambda=k_{j,1,0}+1}^{k_{j,1,1}+3} \sum_{\rho=k_{j,2,0}+1}^{k_{j,2,1}+3} r_{\lambda,\rho} N_{j,4,\rho}(u_2) N_{j,4,\lambda}(u_1),\ u_i \in [2^{-j} k_{j,i,0}; 2^{-j} k_{j,i,1}],\ i = 1, 2$$

where is

$$r_{\lambda,\rho} = \frac{1}{36} f_{\lambda-3,\rho-3} - \frac{2}{9} f_{\lambda-3,\rho-2} + \frac{1}{36} f_{\lambda-3,\rho-1} - \frac{2}{9} f_{\lambda-2,\rho-3} + \frac{16}{9} f_{\lambda-2,\rho-2} - \frac{2}{9} f_{\lambda-2,\rho-1} +$$
$$+ \frac{1}{36} f_{\lambda-1,\rho-3} - \frac{2}{9} f_{\lambda-1,\rho-2} + \frac{1}{36} f_{\lambda-1,\rho-1}. \tag{13}$$

denote

$$R_j = (r_{\lambda,\rho})_{\lambda=k_{j,1,0}+1,\ \rho=k_{j,2,0}}^{k_{j,1,1}+3,k_{j,2,1}+1}; \tag{14}$$

$$\Phi_{j,1}(u_1) = \left(N_{j,4,k_{j,1,0}+1}(u_1) \ldots N_{j,4,k_{j,1,1}+3}(u_1)\right),$$
$$\Phi_{j,2}(u_2) = \left(N_{j,4,k_{j,2,0}+1}(u_1) \ldots N_{j,4,k_{j,2,1}+3}(u_2)\right)$$

Then the function $\tilde{f}$ can be rewritten in the form of [10].

$$\tilde{f}(u_1, u_2) = \Phi_{j,1}(u_1) \cdot R_j \cdot (\Phi_{j,2}(u_2))^T,$$
$$u_i \in [2^{-j}k_{j,i,0}; 2^{-j}k_{j,i,1}], \ i = 1, 2.$$

Let's introduce the kernel of the bundle (the values on the media are specified $[-1; 1] \times [-1; 1] \cap \mathbf{Z}^2$)

$$\tilde{F} = \frac{1}{36}\begin{pmatrix} 1 & -8 & 1 \\ -8 & 64 & -8 \\ 1 & -8 & 1 \end{pmatrix} \tag{15}$$

Then, by definition, there is equality $r_{\lambda,\rho} = (\tilde{F}^- * f)_{\lambda-2,\rho-2}$. Let it be

$$P_{j+1,i} = \frac{1}{8}\begin{pmatrix} 4 & 4 & 0 & \ldots & 0 \\ 1 & 6 & 1 & \ldots & 0 \\ 0 & 4 & 4 & \ldots & 0 \\ 0 & 1 & 6 & \ldots & 0 \\ 0 & 0 & 4 & \ldots & 0 \\ 0 & 0 & 1 & \ldots & 0 \\ \ldots & \ldots & \ldots & \ldots & \ldots \\ 0 & 0 & 0 & \ldots & 4 \end{pmatrix}$$

The size matrix, $(2(k_{j,i,1} - k_{j,i,0}) + 3) \times (k_{j,i,1} - k_{j,i,0} + 3)$, $i = 1, 2$. Then $\Phi_{j,i} = \Phi_{j+1,i} \cdot P_{j+1,i}$.

Consequently,

$$\tilde{f}(u_1, u_2) = \Phi_{j+1,1}(u_1) \cdot (P_{j+1,1} R_j \cdot P_{j+1,2}^T) \cdot (\Phi_{j+1,2}(u_2))^T, \ u_i \in [2^{-j}k_{j,i,0}; 2^{-j}k_{j,i,1}], \ i = 1, 2,$$

Where in $k_{j+1,i,0} = 2k_{j,i,0}$, $k_{j+1,i,1} = 2k_{j,i,1}$, $i = 1, 2$. With this transformation, we obtain approximation functions f on a finer mesh [11]. As follows from formulas (5), in this transformation there is a special case of wavelet recovery. In fig. The 1st example of such a recovery using the example of a test function $f(u_1, u_2) = e^{-\frac{u_1^2+u_2^2}{8}}$, $u_1, u_2 \in [-10; 10]$.

Denote

$$R_{j+l} = (r_{\lambda,\rho}^{(j+l)})_{\lambda=k_{j+l,1,0},\ \rho=k_{j+l,2,0}}^{k_{j+l,1,1},\ k_{j+l,2,1}} = P_{j+l,1} \cdot \ldots \cdot P_{j+1,1} \cdot R_j \cdot P_{j+1,2}^T \ldots P_{j+l,2}^T. \tag{16}$$

Then the locally approximate splint on the grid $\left\{(2^{-j-l}k_1, 2^{-j-l}k_2)\right\}_{(k_1,k_2)\in Z^2}$ has the appearance.

$$\tilde{f}(u_1, u_2) = \Phi_{j+l,1}(u_1) \cdot R_{j+l} \cdot (\Phi_{j+l,2}(u_2))^T, u_i \in [2^{-j-l}k_{j,i,0}; 2^{-j-l}k_{j,i,1}], i = 1, 2$$

We now obtain formulas for calculating the values of the locally approximating spline and its partial derivatives at grid nodes [12, 13]. From the Cox - de Boer relation (9) we find

$$N_{l,4,i}\left(\frac{i-3}{2^l}\right)=\frac{1}{6};N_{l,4,i}\left(\frac{i-2}{2^l}\right)=\frac{2}{3};N_{l,4,i}\left(\frac{i-1}{2^l}\right)=\frac{1}{6};$$
$$N_{l,3,i}\left(\frac{i-2}{2^l}\right)=N_{l,3,i}\left(\frac{i-1}{2^l}\right)=\frac{1}{2},N_{l,2,i}\left(\frac{i-1}{2^l}\right)=1.$$

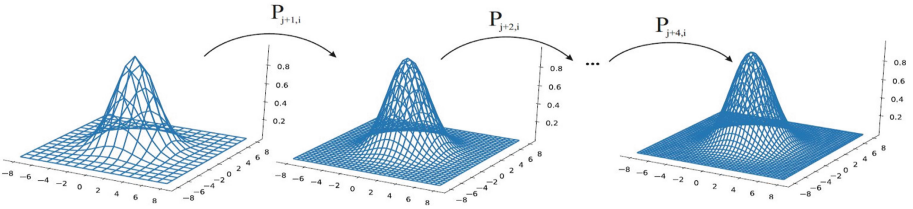

Fig. 1. Vailet-recovery of local-approximation splint.

Therefore, based on the formula (10) we get [14, 15].

$$N'_{l,4,i}\left(\frac{i-3}{2^l}\right)=2^{l-1},N'_{l,4,i}\left(\frac{i-2}{2^l}\right)=0,N'_{l,4,i}\left(\frac{i-1}{2^l}\right)=-2^{l-1};$$
$$N''_{l,4,i}\left(\frac{i-3}{2^l}\right)=2^{2l},N''_{l,4,i}\left(\frac{i-2}{2^l}\right)=-2^{2l+1},N''_{l,4,i}\left(\frac{i-1}{2^l}\right)=2^{2l}.$$

Let's introduce the following bundle kernels (values on the $[-1;1]\times[-1;1]\cap Z^2$ media) [16]:

$$D_{0,0}=\frac{1}{36}\begin{pmatrix}1&4&1\\4&16&4\\1&4&1\end{pmatrix},D_{1,0}=\frac{2^{l-1}}{6}\begin{pmatrix}-1&-4&-1\\0&0&0\\1&4&1\end{pmatrix},D_{0,1}=\frac{2^{l-1}}{6}\begin{pmatrix}-1&0&1\\-4&0&4\\-1&0&1\end{pmatrix},$$
$$D_{1,1}=2^{2l-2}\begin{pmatrix}1&0&-1\\0&0&0\\-1&0&1\end{pmatrix},D_{2,0}=\frac{2^{2l}}{6}\begin{pmatrix}1&4&1\\-2&-8&-2\\1&4&1\end{pmatrix},D_{0,2}=\frac{2^{2l}}{6}\begin{pmatrix}1&-2&1\\4&-8&4\\1&-2&1\end{pmatrix}.$$

Then the $\tilde{f}$ following equalities are fair for the values of the locally approximately splined and its private derivatives in the nodes $\left(\frac{\lambda}{2^{j+l}},\frac{\rho}{2^{j+l}}\right)$ grids [12, 13]. From the Cox - de Boer relation (9) we find

$$D^{(d_1,d_2)}\tilde{f}\left(2^{-j-l}\lambda,2^{-j-l}\rho\right)=D^{-}_{d_1,d_2}*R_{j+l}(\lambda+2,\rho+2),$$
$$d_1,d_2=0,1,2,\quad d_1+d_2\le 2;\quad \lambda=k_{j+l,1,0},\ldots,k_{j+l,1,1},\quad \rho=k_{j+l,2,0},\ldots,k_{j+l,2,1}. \tag{17}$$

4 Algorithms App

One of the methods for producing structures from composite materials is the automated calculation method, in which tapes are placed on the surface of the technological mandrel using pressure rollers [17, 18].

The surface of the fan blade is defined by some sets of points in several sections. First, we model this surface using a locally approximating spline of two variables [19]. Then we find the values of this spline at the nodes of the finer mesh and shift the surface points corresponding to these nodes normal to the surface by a height equal to the thickness of the tape. Next, we carry out the wavelet decomposition with zeroing the wavelet coefficients. As a result, surface smoothing occurs [20].

5 Conclusion

The article presents computational algorithms for locally approximating splines based on the use of the inverse discrete wavelet transform and convolution transform. The algorithms are applied to the development of a part of the CAD system for the manufacture of structures from composite materials by automated calculation.

References

1. Deniskin, Y., Miroshnichenko, P., Smolyaninov, A.: Geometric modeling of surfaces dependent cross sections in the tasks of spinning and laying. In: E3S Web of Conferences (2019). https://doi.org/10.1051/e3sconf/201911001057
2. Todorova, M., Parvanova, R.: Biorthogonal wavelet filtration of signals used in the industrial automation systems. In: 16th Conference on Electrical Machines, Drives and Power Systems (2019). https://doi.org/10.1109/ELMA.2019.8771662
3. Pocebneva, I., Deniskin, Y., Yerokhin, A.: Simulation of an aerodynamic profile with sections of ad hoc concavity. In: E3S Web of Conferences, vol. 110, p. 01074 (2019)
4. Bityukov, Y., Platonov, E.N.: The use of wavelets to calculate linear control systems with lumped parameters. Inf. Appl. **11**, 4 (2017)
5. Bityukov, Y., Kalinin, V.A.: Application of wavelets in computer-aided design systems. Electronic Journal Proceedings of the MAI, p. 84 (2015)
6. Bityukov, Y.I., Deniskin, Y.I., Pocebneva, I.V.: Construction of smooth biorthogonal waves on triangulated spaces. In: International Russian Automation Conference 2019 (2019). https://doi.org/10.1109/RUSAUTOCON.2019.8867785
7. Matys, E., Deniskin, Y., Stativa, E., et al.: Special features of obtaining fine powders for additive technologies. In: E3S Web of Conferences (2019). https://doi.org/10.1051/e3sconf/201911001057
8. Artamonov, I.M., Deniskina, A.R., Deniskin, Y.: Formation of a single information object for targeted solutions in the aerospace industry. In: Salenko, S.D. (ed.) Science Industry Defense Proceedings of the XIX All-Russian Scientific and Technical Conference, pp. 57–61 (2018)
9. Bityukov, Y.I., Deniskin, Y.I.: Chaikin algorithm and its generalization. Dynamics of systems, mechanisms and machines. Dynamics 7818981 (2016)
10. Kiselev, E.A., Minin, L.A., Novikov, I.Y.: On the construction of biorthogonal systems for subspaces generated by integral shifts of a single function. Math. Notes **96**(3–4), 451–453 (2014). https://doi.org/10.1134/S000143461409017X

11. Zhang, B., Zheng, H., Zhou, J., et al.: Construction of a family of non-stationary biorthogonal wavelets. J. Inequalities Appl. **1** (2019). https://doi.org/10.1186/s13660-019-2240-2
12. Mohammad, M.: Biorthogonal-wavelet-based method for numerical solution of Volterra integral equations. Entropy **21**(11), 1098 (2019). https://doi.org/10.3390/e21111098
13. Mayeli, A., Wavelets, R.: Tiling and spectral sets in LCA groups, complex analysis and operator theory **13**(3), 1177–1195 (2017). https://doi.org/10.1007/s11785-018-0843-0
14. Makarov, A., Makarova, S.: On lazy Faber's type decomposition for linear splines. AIP Conf. Proc. (2019). https://doi.org/10.1063/1.5130851
15. Bityukov, Y., Akmaeva, V.N.: The use of wavelets in the mathematical and computer modelling of manufacture of the complex-shaped shells made of composite materials. Bull. South Ural State Univ. Math. Modell. Program. Comput. Softw. **9**(3), 5–16 (2016)
16. Lepik, U., Hein, H.: Haar Wavelets with Applications. Springer, Berlin (2014)
17. Bityukov, Y.I., Deniskin, Y.I., Deniskina, G.Y.: Spline wavelets use for output processes analysis of multi-dimensional non-stationary linear control systems. J. Phys. Conf. Ser. **944**(1), 012018 (2017)
18. Qin, Y., Mao, Y., Tang, B., et al.: M-band flexible wavelet transform and its application to the fault diagnosis of planetary gear transmission systems. Mech. Syst. Sign. Process. (2019). https://doi.org/10.1016/j.ymssp.2019.106298
19. Kale, M.C.: A general biorthogonal wavelet based on Karhunen-Loeve transform approximation. Sign. Image Video Process. **10**(4), 791–794 (2016). https://doi.org/10.1007/s11760-016-0860-2
20. Anoh, O.O., Abd-Alhameed, R.A., Jones, S.M., et al.: Comparison of orthogonal and biorthogonal wavelets for multicarrier systems. In: 8th IEEE Design and Test Symposium (2013). https://doi.org/10.1109/IDT.2013.6727137